REPORT No. 607

SPINNING CHARACTERISTICS OF THE XN2Y–1 AIRPLANE OBTAINED FROM THE SPINNING BALANCE AND COMPARED WITH RESULTS FROM THE SPINNING TUNNEL AND FROM FLIGHT TESTS

By M. J. Bamber and R. O. House

SUMMARY

A 1/10-scale model of the XN2Y–1 airplane was tested in the N. A. C. A. 5-foot vertical wind tunnel and the six components of the forces and moments were measured. The model was tested in 17 attitudes in which the full-scale airplane had been observed to spin, in order to determine the effects of scale, tunnel, and interference. In addition, a series of tests was made to cover the range of angles of attack, angles of sideslip, rates of rotation, and control settings likely to be encountered by a spinning airplane. The data were used to estimate the probable attitudes in steady spins of an airplane in flight and of a model in the free-spinning tunnel.

The estimated attitudes of steady spin were compared with attitudes measured in flight and in the spinning tunnel. The results indicate that corrections for certain scale and tunnel effects are necessary to estimate full-scale spinning attitudes from model results.

INTRODUCTION

General methods for the theoretical analysis of airplane spinning characteristics have been available for some time. These methods might be used by designers to predict the spinning characteristics of proposed airplane designs if the necessary aerodynamic data were known.

In order to provide these data, the N. A. C. A. is conducting investigations to determine the aerodynamic forces and moments on airplane models and on the various parts of airplane models in spinning attitudes. This report gives a comparison of the results obtained for a model on the spinning balance with those for the airplane in full-scale spins and for a model in the free-spinning tunnel. The XN2Y–1 is the first airplane to be tested for comparative purposes in these three ways. The flight tests are reported in references 1 and 2, the results from the free-spinning tunnel in reference 3, and those from the spinning balance are given in this report. Flight and spinning-balance results have been compared for two other airplanes. (See references 4 and 5.)

The present report gives the aerodynamic forces and moments acting on the XN2Y–1 airplane model for the range of probable spinning attitudes with various rudder, elevator, and aileron deflections and in 17 specific attitudes in which the full-scale airplane had been observed to spin. These forces and moments are also given for parts of the model for the 17 flight attitudes. An analysis of the data and a discussion of the results of the analysis with respect to flight results and to model tests in the free-spinning tunnel are included.

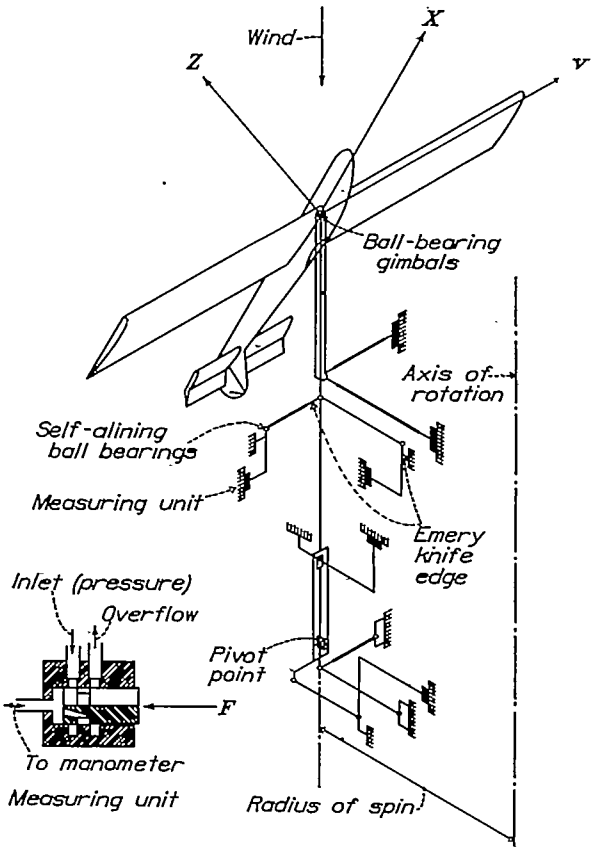

FIGURE 1.—Line diagram of spinning-balance force system.

APPARATUS AND MODELS

The tests were made in the N. A. C. A. 5-foot vertical open-jet wind tunnel described in reference 6.

The 6-component balance, as described in reference 4, was altered to give more accurate results and to allow for more rapid testing. The balance force system, as modified to give more accurate readings, is shown in figure 1. A sleeve to which the model is attached was installed over the upper end of the vertical spindle, is fastened to the spindle by a ball-bearing gimbal joint

at the upper end, and is held in position by linkages to two measuring units at its lower end. This arrangement allows the rolling and pitching moments (earth axes) to be measured directly instead of being the small algebraic sum of two and three relatively large measurements. Consequently, much greater accuracy may be obtained with the same variations in balance readings so that fewer repeat tests are necessary.

This alteration and the direct-indicating force-measuring system that was installed have reduced the time required to obtain data. The force-measuring system consists of an oil pump and six mercury manometers outside the tunnel, seven slip joints on the lower end of the turntable shaft, and six measuring units on the balance head. Each measuring unit consists of a grooved piston and cylinder and is shown by the small sketch in figure 1.

The principle of operation is that the force (see F in fig. 1) applied to the piston is balanced by oil pressure in the cylinder. The grooves in the cylinder and in the piston act as balanced valves, allowing oil to flow into or out of the cylinder, depending on the location of the piston in the cylinder. The oil pressure acting on the piston in the closed end of the cylinder is transmitted through a slip joint and is indicated by the mercury manometer.

One oil-pressure line from the pump and one overflow line connect to all six measuring units. Each unit is connected through a slip joint to a mercury manometer; each manometer is provided with a shut-off valve; and all the valves are operated at the same time so that all the readings are made simultaneously.

The model, a 1/10-scale reproduction of the XN2Y-1 airplane, was made from dimensions obtained from the airplane as used for tests in reference 2. Figure 2 shows it mounted on the balance in the tunnel. The model differed from the airplane principally in that it had no propeller, the struts were round rods, and the fuselage and the trailing-edge center section of the upper wing were cut away for attachment to the balance. The model also differed from the airplane, as tested in reference 1, in that the airplane had the fin offset and the fabric sagged between the ribs. The wings, fuselage, wheels, and stabilizer of the model were of mahogany, the struts of 3/32-inch brass rod, and the fin, rudder, and elevator of duralumin. The wings and the fuselage mounted separately are shown in figures 3 and 4. A small streamline fuselage section was used to attach the wings to the balance. The tolerances allowed for the construction were: Wing profile, ± 0.003 inch; fuselage cross section, ± 0.005 inch; tail surfaces, ± 0.003 inch; other dimensions generally, ± 0.01 inch; and angular relationships, $\pm 0.1°$.

TESTS

Tests were made at 40°, 50°, 60°, and 70° angle of attack. At each angle of attack tests were made at $-10°$, 0°, 5°, and 15° angle of sideslip. At each angle of attack at each angle of sideslip, tests were made with values of $\Omega b/2V$ of 0.35, 0.50, 0.75, and 1.00. For each attitude tests were made with the elevator up, rudder with spin; elevator neutral, rudder neutral; and elevator down, rudder against the spin. For each attitude with elevator up, rudder with the spin, except zero sideslip, tests were made with ailerons with and against the spin. Tests were made with elevator up, ailerons neutral, and rudder positions of 40°, 25°, 17°, 8°, and 0° with the spin at $\alpha=60°$, $\Omega b/2V=0.75$, $\beta=0°$ and 15°; and at $\alpha=50°$, $\Omega b/2V=0.50$, and $\beta=5°$ and $-10°$.

The control-surface angles for the various settings were:

Elevator up	elevators 23° 41′ up.
Elevator down	elevators 25° down.
Rudder with	rudder 40° to aid the rotation.
Rudder against	rudder 40° to oppose the rotation.
Aileron with	ailerons displaced to increase the rolling.
Aileron against	ailerons displaced to oppose the rolling.

Aileron deflections were 25° up and 15° down, both ailerons being deflected in each case.

The radius of the spin for each attitude was computed from an equilibrium of centrifugal and aerodynamic forces. The normal weight of the airplane was used and the aerodynamic forces were obtained from the data in reference 7. The resultant force on the airplane was assumed to be perpendicular to the XY plane.

Tests were also made in 17 specific attitudes obtained from measurements of full-scale spins. Table I gives the attitudes and control positions.

TABLE I.—AIRPLANE ATTITUDES AS TESTED ON THE SPINNING BALANCE

[Tests 44L through 109L from reference 1. Tests 29F through 36 from reference 2. All values have been given proper signs for right spins. Right and left spins given in references 1 and 2. In a right spin inward sideslip is positive.]

Flight test	α (deg.)	β (deg.)	$\frac{\Omega b}{2V}$	δ_r (deg.)	δ_e (deg.) (min.)	δ_a (deg.)	Radius (ft.)
44L	53.1	−0.8	0.554	−40	−25 30	0	2.60
52L	50.1	1.0	.453	−40	−25 30	0	3.70
77L	70.7	9.0	.838	−40	−25 30	0	1.30
84L	69.1	7.4	.970	−40	−25 30	0	.60
107L	57.0	10.8	.753	−40	−25 30	With	1.70
109L	65.5	9.8	.853	−40	−25 30	Against	.91
29F	60.7	13.7	.593	−40	−23 50	0	1.60
29G	60.4	13.0	.622	−40	−23 50	0	1.60
20	50.6	4.3	.598	−40	26 35	0	2.00
30	52.4	1.0	.535	−40	26 35	0	2.30
33	40.2	4.4	.534	0	−23 50	0	2.70
31	48.6	−1.9	.390	−17	−23 50	0	3.50
32C	47.0	.9	.437	−4	−23 50	0	3.90
34B	44.4	.4	.414	−4	−23 50	0	4.00
27B	43.0	3.9	.411	−8	−23 50	0	4.70
35	57.4	9.7	.523	−18	−23 50	0	2.20
36	50.9	.6	.393	−40	26 35	0	2.30

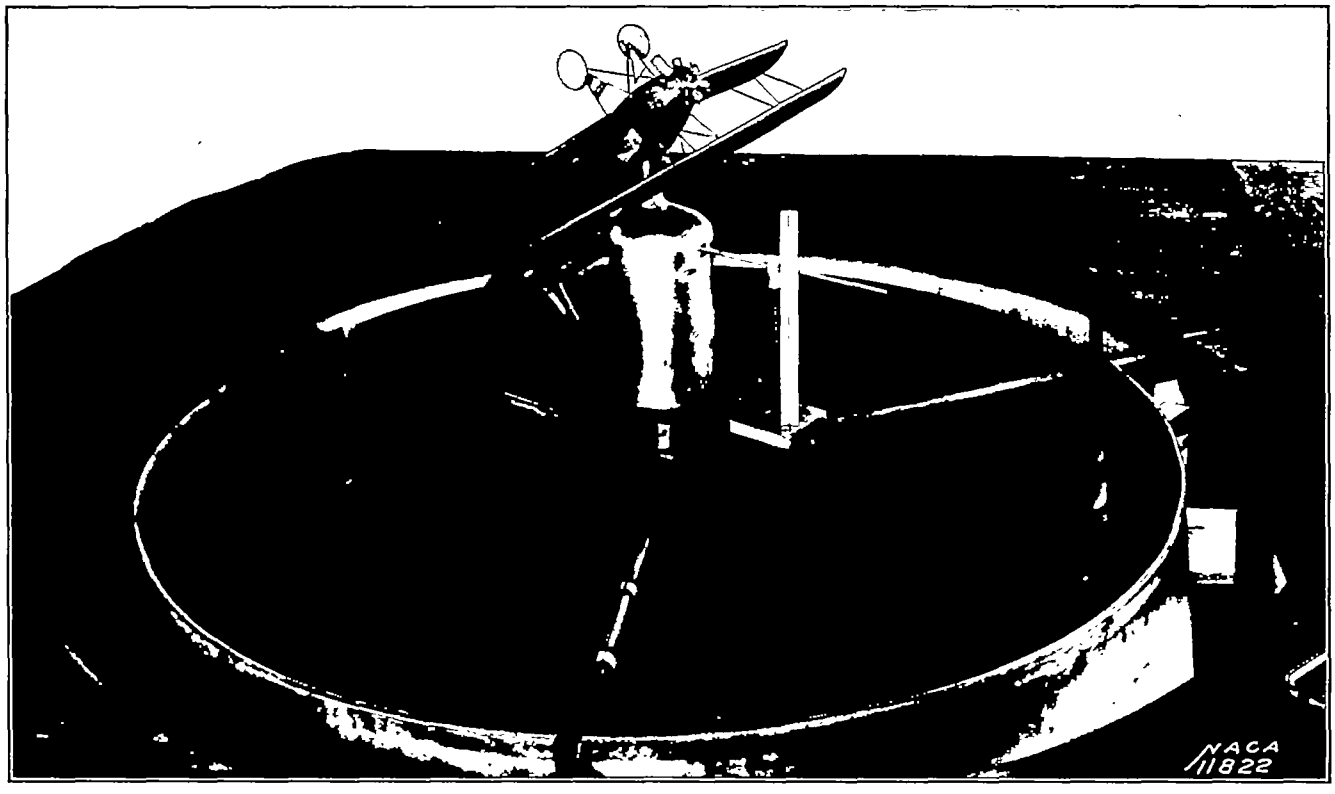

FIGURE 2.—The XN2Y-1 airplane model mounted on the spinning balance.

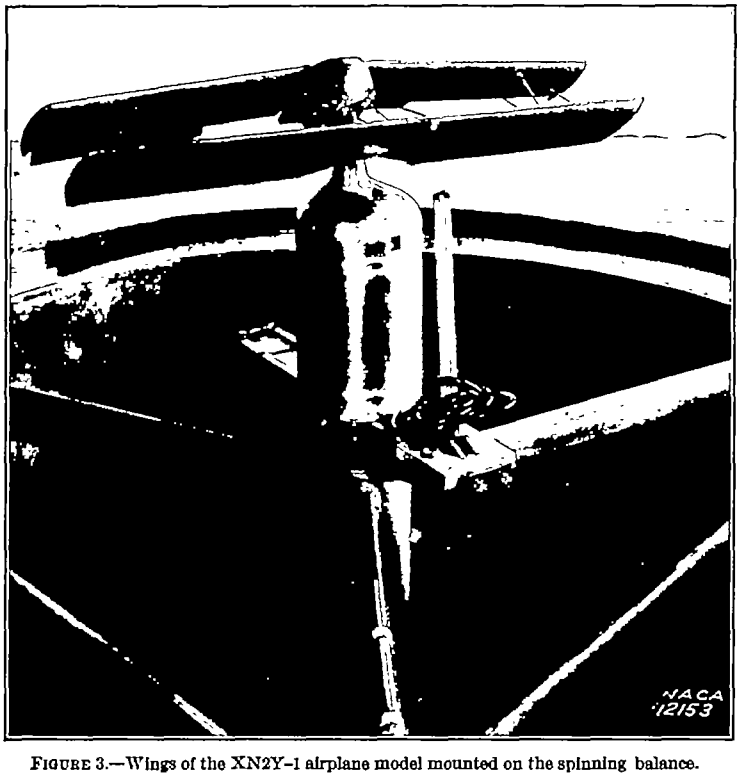

FIGURE 3.—Wings of the XN2Y-1 airplane model mounted on the spinning balance.

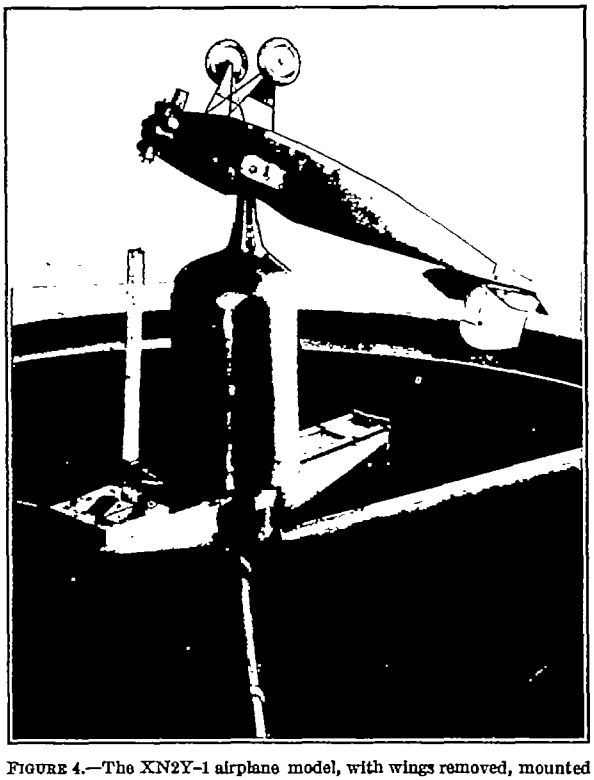

FIGURE 4.—The XN2Y-1 airplane model, with wings removed, mounted on the spinning balance.

The model was not changed for the test corresponding to those given in reference 1, in which the airplane had the fin offset and the original wing profile on which the fabric sagged between the ribs. For each test the controls were set the same as for the flight spins. In each attitude tests were made with the model complete, with the fin and rudder removed, with the wings removed, and with the wings alone. (See figs. 3 and 4.)

In order to insure consistency of results, repeat tests were made for each condition until individual balance readings were found to agree within a specified limit or until a sufficient number of readings had been made to form a fair average. In each case an average of the results obtained was used to obtain the coefficients. The air speeds for the tests varied between 43 and 75 feet per second and covered a range of test Reynolds Numbers from about 100,000 to 175,000. Early tests on the spinning balance indicated no scale effects over this speed range (reference 4). The lower air speeds were used with the larger values of $\Omega b/2V$ because of the necessarily high rate of rotation.

SYMBOLS

α, angle of attack at center of gravity.

$\beta=\sin^{-1}\frac{v}{V}$, angle of sideslip at the center of gravity.

V, resultant linear velocity of the center of gravity.

v, linear velocity along the Y airplane axis, positive when the airplane is sideslipping to the right.

Ω, resultant angular velocity (radians per second).

δ_a, aileron deflection.

δ_e, elevator deflection.

δ_r, rudder deflection.

σ, angle between the vertical and the helix described by the center of gravity of the airplane.

b, span of wing.

S, area of wing.

$q=1/2\ \rho V^2$, dynamic pressure.

ρ, air density.

X, longitudinal force acting along the X airplane axis, positive forward.

Y, lateral force acting along the Y airplane axis, positive to the right.

Z, normal force acting along the Z airplane axis, positive downward.

L, rolling moment acting about the X airplane axis, positive when it tends to lower the right wing.

M, pitching moment acting about the Y airplane axis, positive when it tends to increase the angle of attack.

N, yawing moment acting about the Z airplane axis, positive when it tends to turn the airplane to the right.

Forces and moments with double primes (e. g., X'') are in the earth system of axes where Z'' is positive downward and X'' is along the radius of the spin, positive toward the center of the spin.

Coefficients of forces are obtained by dividing the force by qS.

Coefficients of moments are obtained by dividing the moment by qbS.

$\mu=\frac{m}{\rho Sb}$, relative density of airplane to air. Under standard conditions, $\mu=13.1\ W/Sb$.

$m=W/g$, mass.

k_X, k_Y, k_Z, radii of gyration of the airplane about the X, Y, and Z airplane axes, respectively.

$\frac{b^2}{k_Z^2-k_X^2}=\frac{Wb^2}{g(C-A)}$, pitching-moment inertia parameter.

$\frac{k_Z^2-k_Y^2}{k_Z^2-k_X^2}=\frac{C-B}{C-A}$, rolling-moment and yawing-moment inertia parameter.

$A=mk_X^2$, moment of inertia about the X airplane axis.

$B=mk_Y^2$, moment of inertia about the Y airplane axis.

$C=mk_Z^2$, moment of inertia about the Z airplane axis.

RESULTS

Results of the measurements have been reduced to the following coefficient forms, which are standard except that of the pitching moment, for which the coefficient is based on the span of the wing:

$$C_X=\frac{X}{qS} \qquad C_Y=\frac{Y}{qS} \qquad C_Z=\frac{Z}{qS}$$

$$C_l=\frac{L}{qbS} \qquad C_m=\frac{M}{qbS} \qquad C_n=\frac{N}{qbS}$$

Pitching-moment coefficients can be referred to the chord of the wing by multiplying the values given by 7.47. All values of the coefficients are given with proper signs for right-hand spins. The values of the coefficients for the series of tests are given in figures 5 to 9. Variations of C_l, C_m, and C_n with β, $\Omega b/2V$, and control settings for some characteristic cases are shown in figures 10 to 22.

The differences between the coefficients of flight and model results (flight minus model) are given in figures 23 to 26. The values of C_n for parts of the airplane (reference 2) and of the model are given in figure 27. The values of $\sqrt{C_{X''}^2+C_{Y''}^2}$ (or $C_{X''}$) C_l, C_m, and C_n for the airplane and for the model, and the values obtained by adding the coefficients of the wings tested separately to those of the model with the wings removed, are given in figures 28 to 31.

The data given are believed to be correct for the model under the conditions of the tests within the following limits:

C_Z, ± 0.02	C_m, ± 0.002
C_l, ± 0.001	C_n, ± 0.001

No corrections have been made for tunnel-wall, blocking, or scale effects. The interference caused by the balance parts would appear to be large, especially at 40° angle of attack where the tail surfaces were very near the balance, as is shown by figure 2. Interference effects, however, are not obvious in the results given in figures 23 to 31.

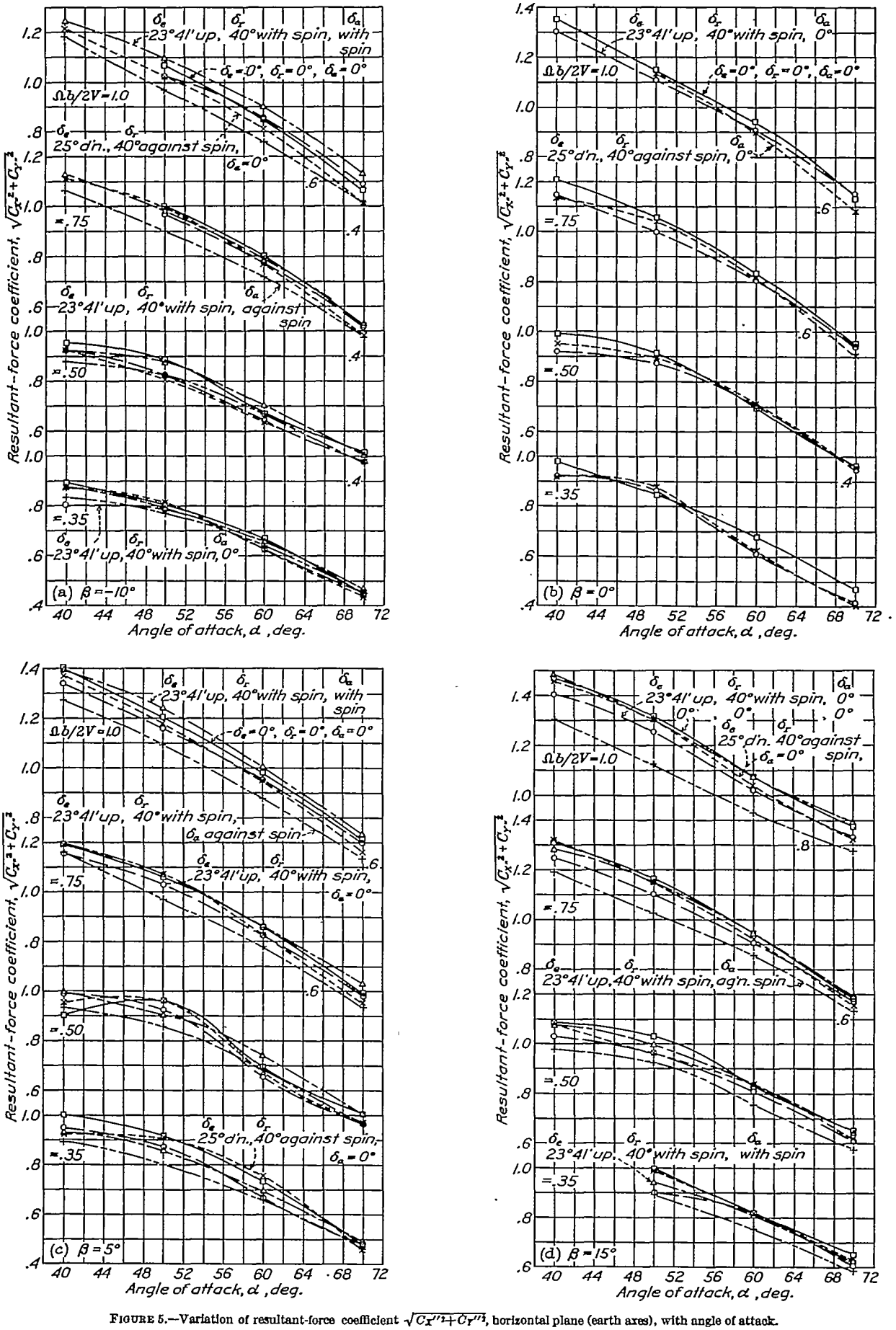

FIGURE 5.—Variation of resultant-force coefficient $\sqrt{C_{X'}^2+C_{Y'}^2}$, horizontal plane (earth axes), with angle of attack.

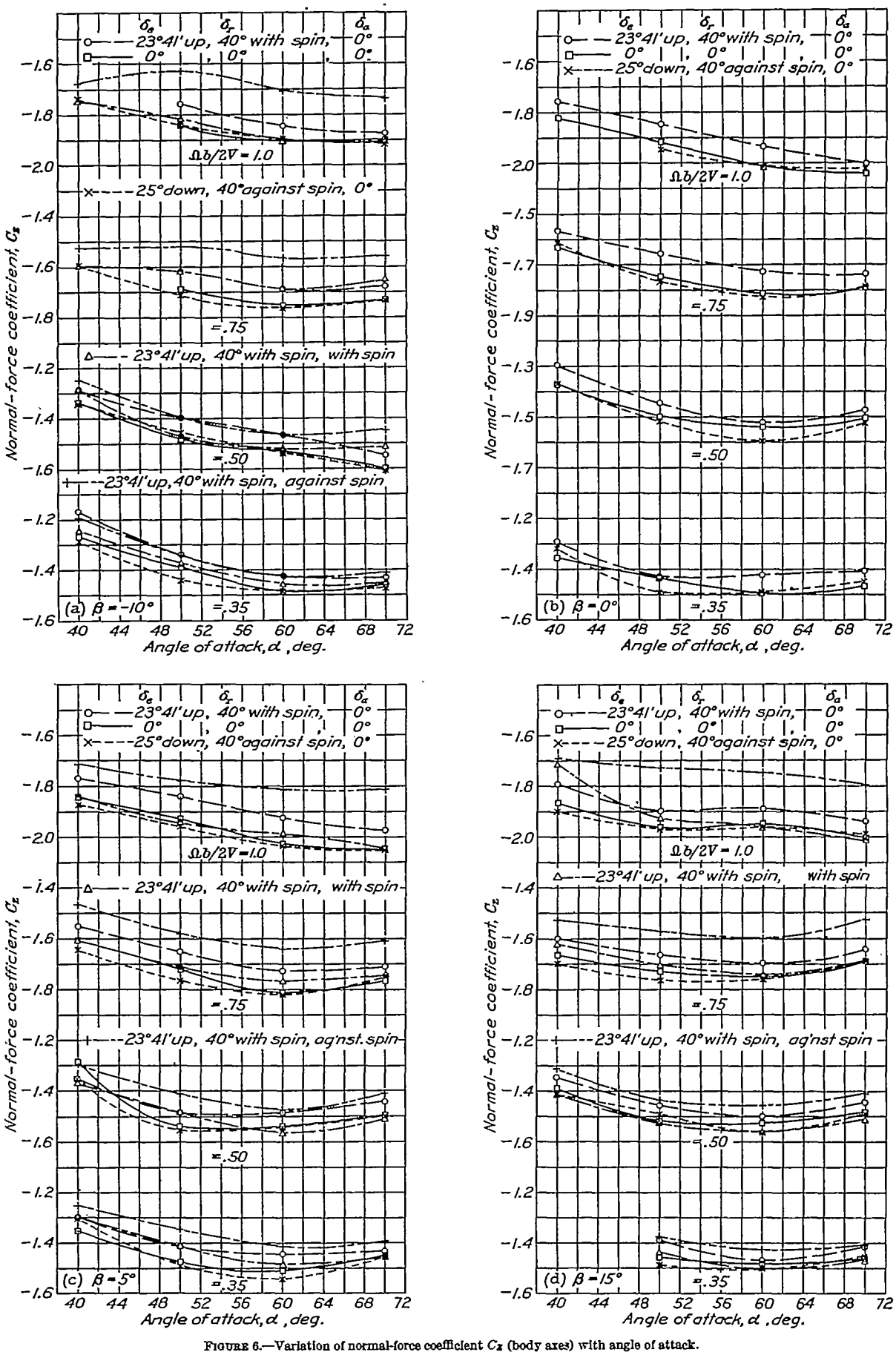

FIGURE 6.—Variation of normal-force coefficient C_z (body axes) with angle of attack.

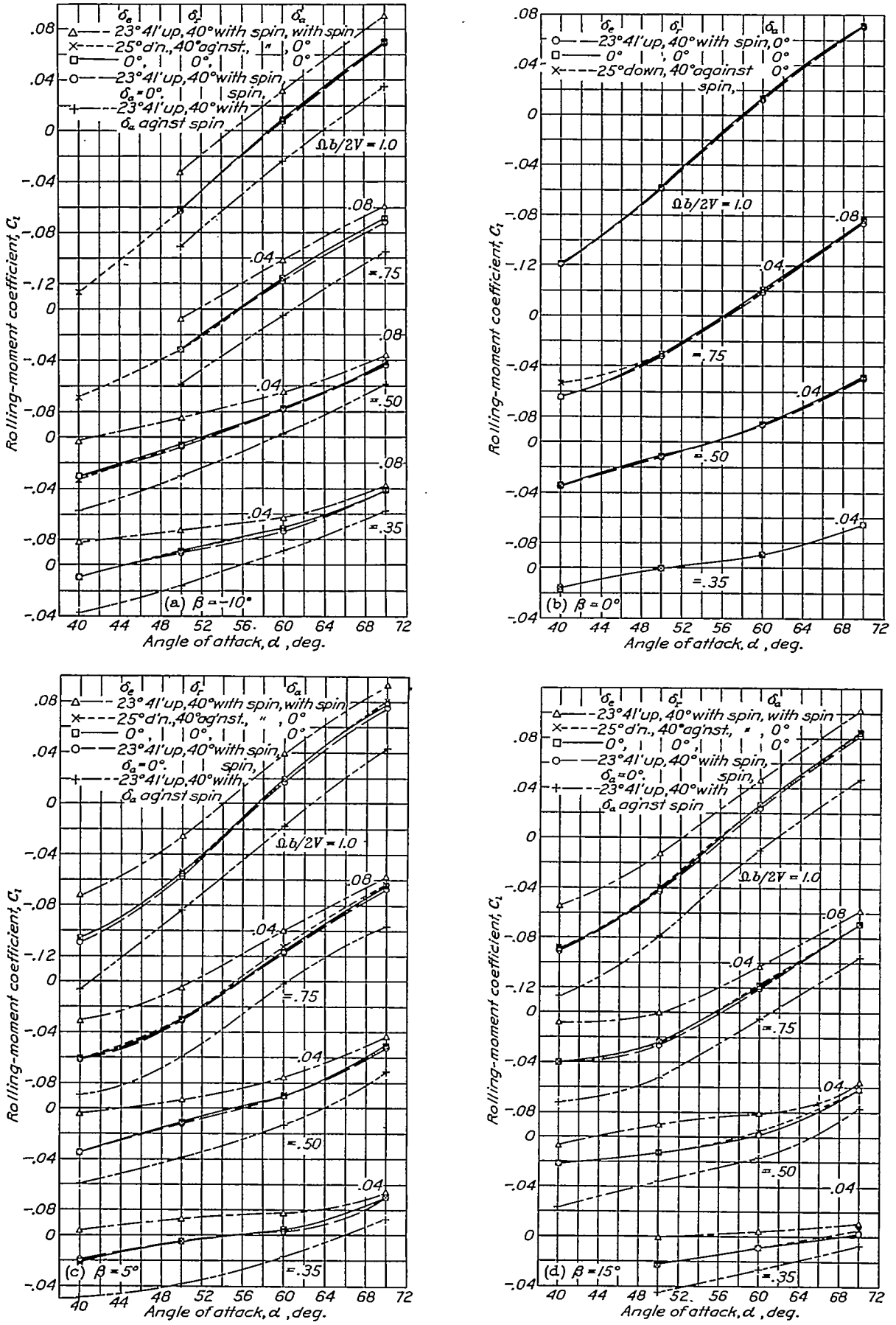

FIGURE 7.—Variation of rolling-moment coefficient C_l (body axes) with angle of attack.

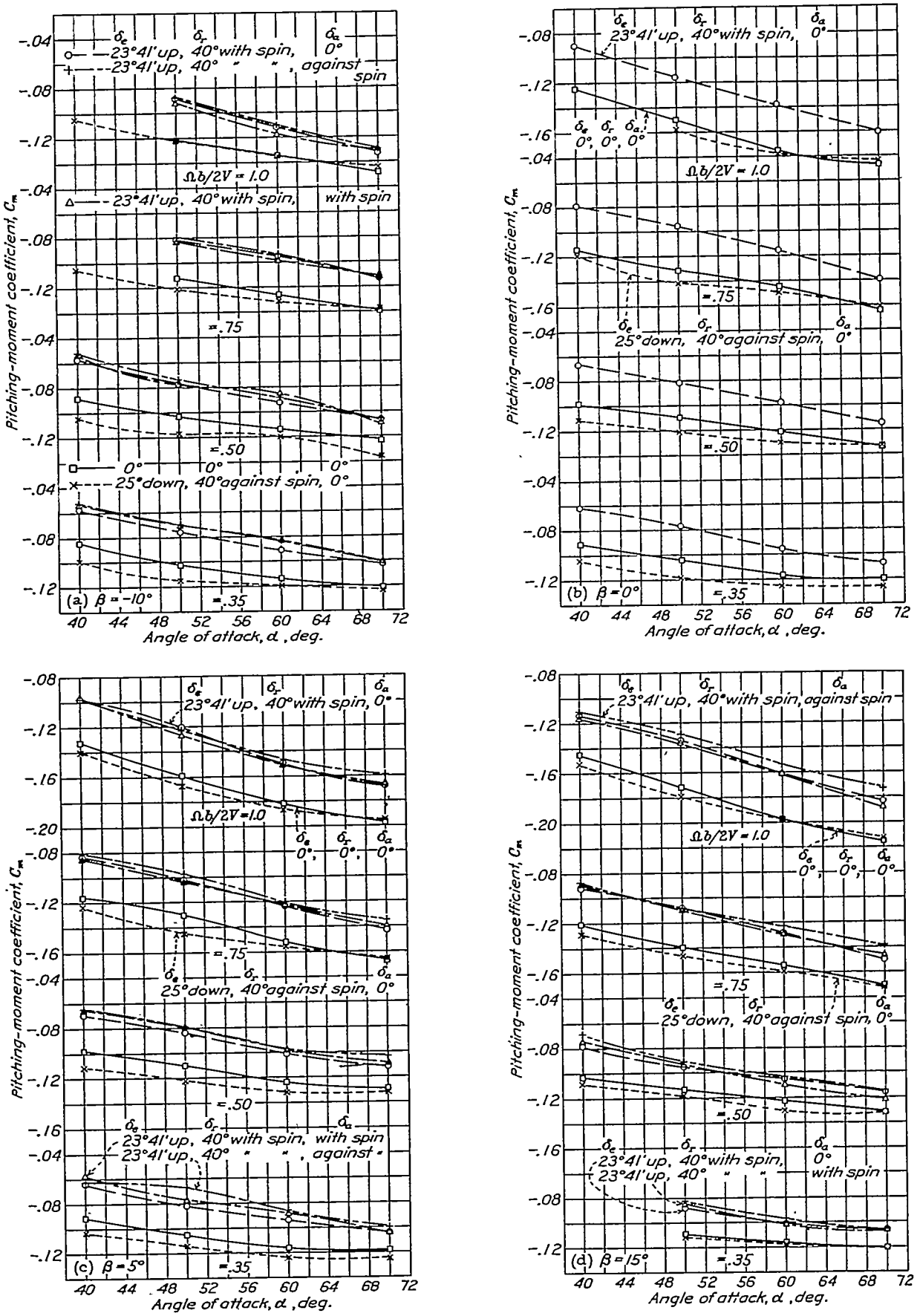

FIGURE 8.—Variation of pitching-moment coefficient C_m (body axes) with angle of attack.

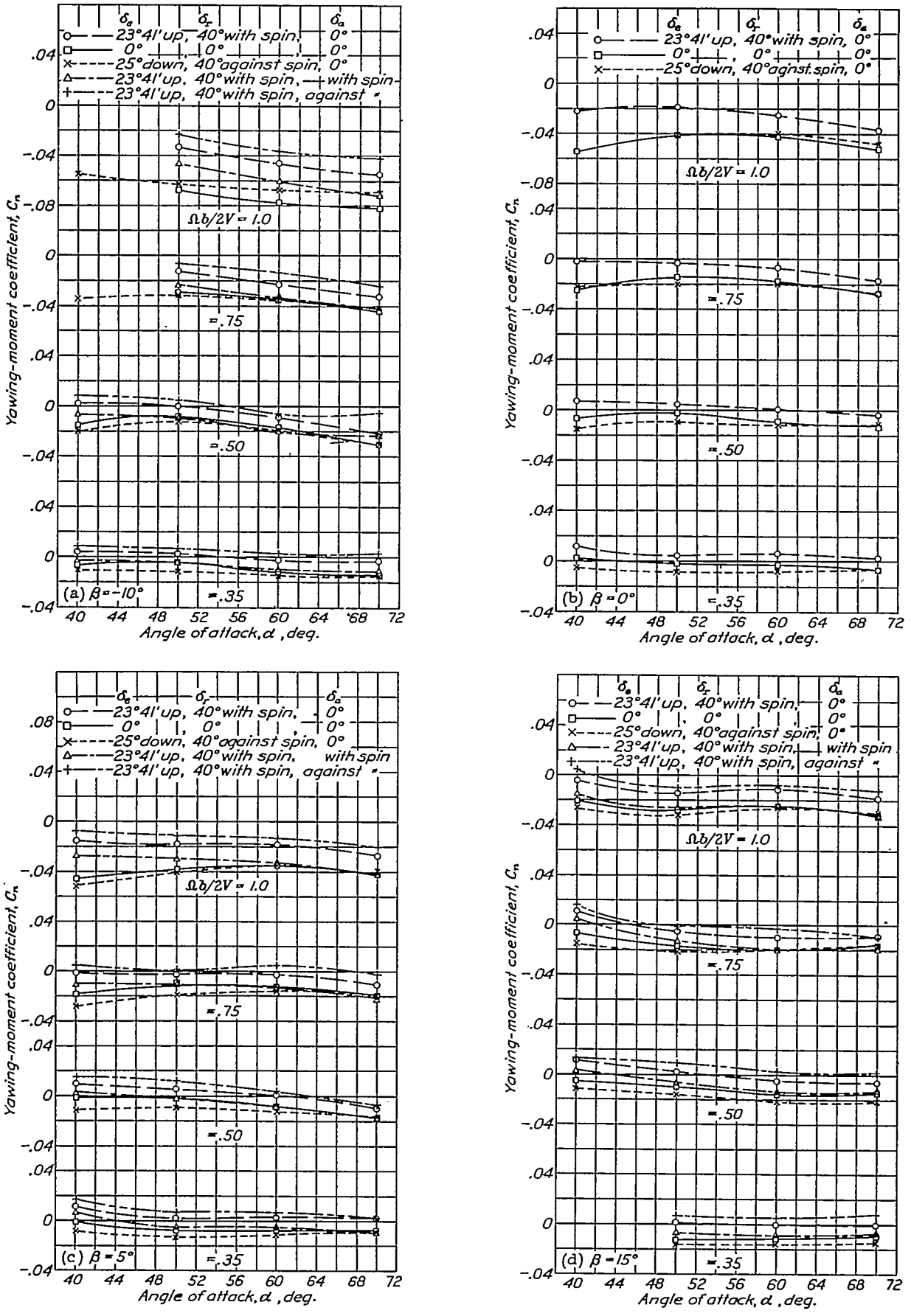

FIGURE 9.—Variation of yawing-moment coefficient C_n (body axes) with angle of attack.

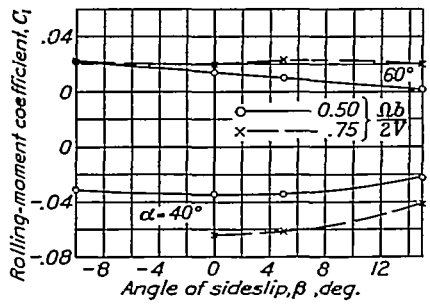

FIGURE 10.—Variation of rolling-moment coefficient C_l (body axes) with angle of sideslip. $\delta_a=0°$; $\delta_e=23°41'$ up; $\delta_r=40°$ with spin.

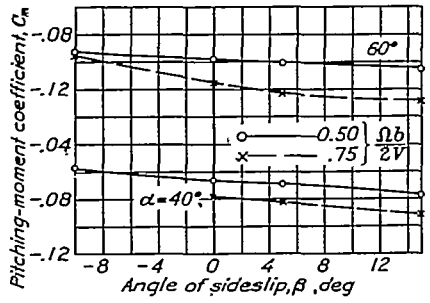

FIGURE 11.—Variation of pitching-moment coefficient C_m (body axes) with angle of sideslip. $\delta_a=0°$; $\delta_e=23°41'$ up; $\delta_r=40°$ with spin.

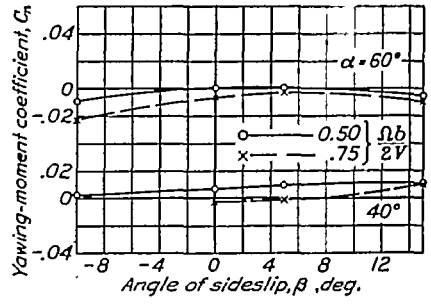

FIGURE 12.—Variation of yawing-moment coefficient C_n (body axes) with angle of sideslip. $\delta_a=0°$; $\delta_e=23°41'$ up; $\delta_r=40°$ with spin.

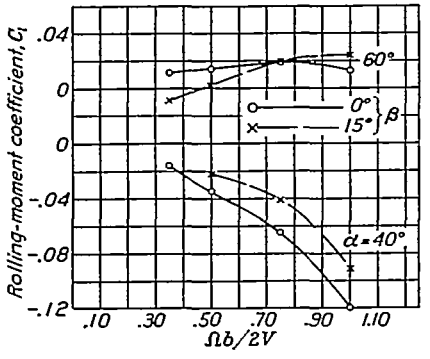

FIGURE 13.—Variation of rolling-moment coefficient C_l (body axes) with $\Omega b/2V$. $\delta_a=0°$; $\delta_e=23°41'$ up; $\delta_r=40°$ with spin.

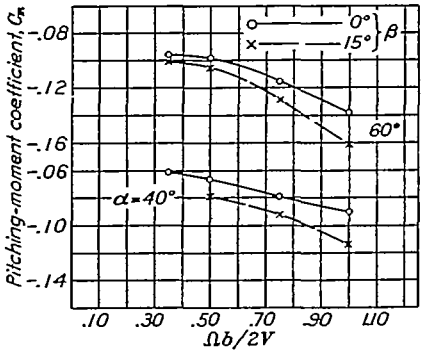

FIGURE 14.—Variation of pitching-moment coefficient C_m (body axes) with $\Omega b/2V$. $\delta_a=0°$; $\delta_e=23°41'$ up; $\delta_r=40°$ with spin.

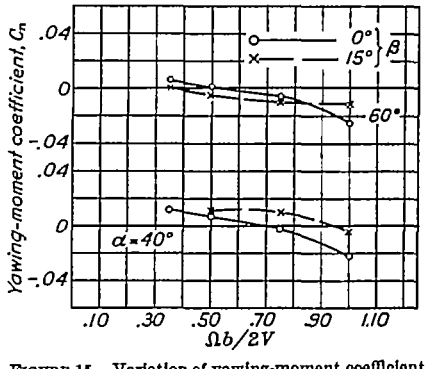

FIGURE 15.—Variation of yawing-moment coefficient C_n (body axes) with $\Omega b/2V$. $\delta_a=0°$; $\delta_e=23°41'$ up; $\delta_r=40°$ with spin.

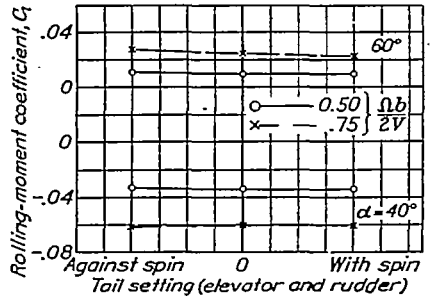

FIGURE 16.—Variation of rolling-moment coefficient C_l (body axes) with tail setting. $\beta=5°$; $\delta_a=0°$.

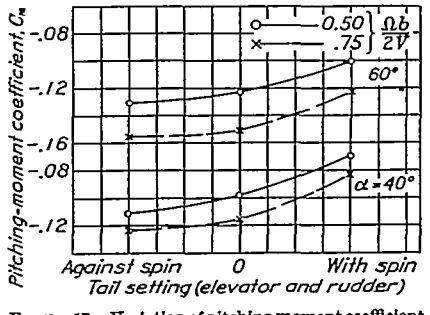

FIGURE 17.—Variation of pitching-moment coefficient C_m (body axes) with tail setting. $\beta=5°$; $\delta_a=0°$.

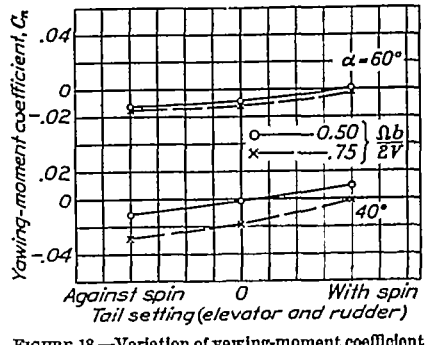

FIGURE 18.—Variation of yawing-moment coefficient C_n (body axes) with tail setting. $\beta=5°$; $\delta_a=0°$.

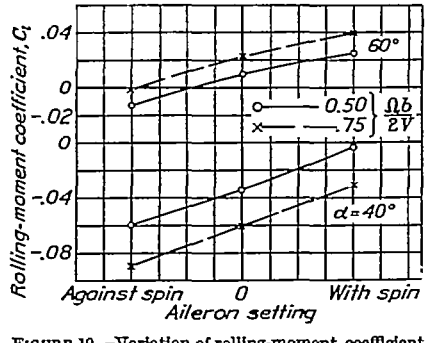

FIGURE 19.—Variation of rolling-moment coefficient C_l (body axes) with aileron setting. $\beta=5°$; $\delta_a=23°41'$ up; $\delta_r=40°$ with spin.

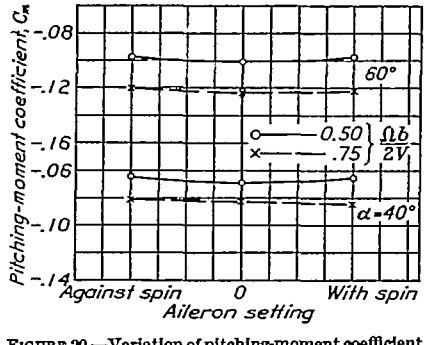

FIGURE 20.—Variation of pitching-moment coefficient C_m (body axes) with aileron setting. $\beta=5°$; $\delta_a=23°41'$ up; $\delta_r=40°$ with spin.

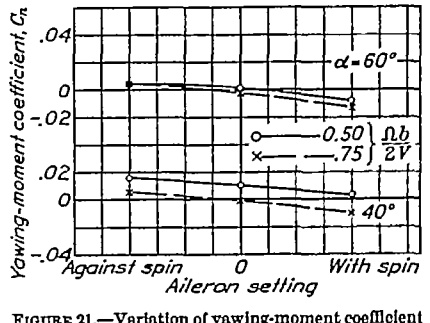

FIGURE 21.—Variation of yawing-moment coefficient C_n (body axes) with aileron setting. $\beta=5°$; $\delta_a=23°41'$ up; $\delta_r=40°$ with spin.

DISCUSSION OF DATA

General series of tests.—The values of $\sqrt{C_{X''}^2+C_{Y''}^2}$ (fig. 5) are given because they were used in the analysis. The values of C_X and C_Y are not given because they are small and are probably of no importance for any analysis of the data.

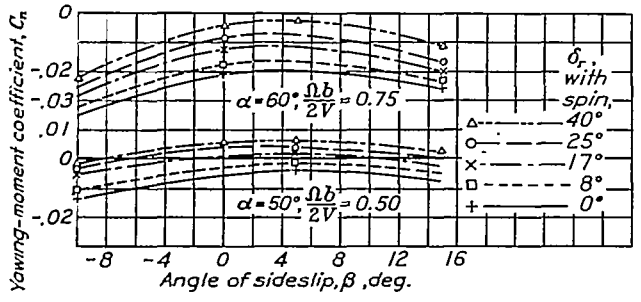

FIGURE 22.—Variation of yawing-moment coefficient C_n (body axes) with rudder setting. $\delta_a = 0°$; $\delta_e = 23°41'$ up.

Comparison of coefficients from model and flight results.—The difference in the coefficients in the horizontal plane (fig. 23) is irregular but shows a general tendency to be slightly negative (model results smaller than flight).

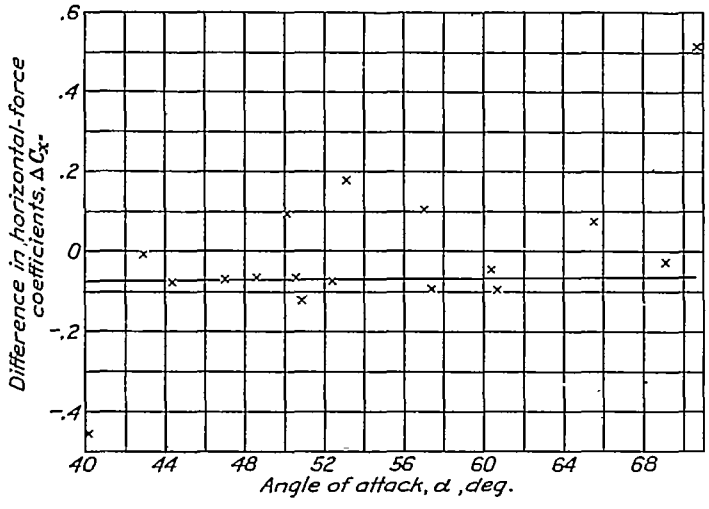

FIGURE 23.—Variation of difference in horizontal-force coefficients of airplane and model $\Delta C_{X''}$ (earth axes) with angle of attack.

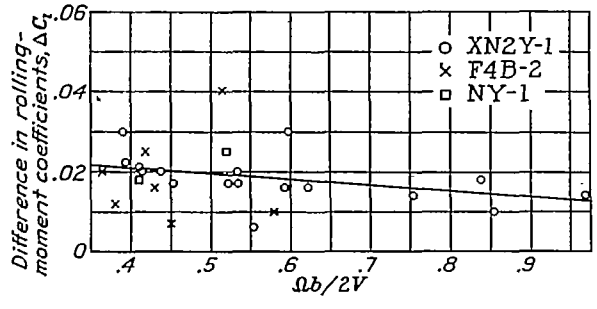

FIGURE 24.—Variation of difference in rolling-moment coefficients of airplane and model ΔC_l (body axes) with $\Omega b/2V$.

The difference in the rolling-moment coefficients ΔC_l shows no general tendency to vary with α or β but shows a slight tendency to decrease as $\Omega b/2V$ is increased (fig. 24). The average value is 0.02, the same as that found for the NY–1 and F4B–2 airplanes (references 4 and 5). The individual values of ΔC_l for the NY–1 and F4B–2 airplanes are given in figure 24.

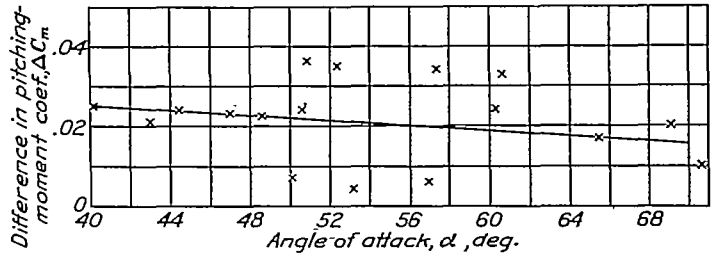

FIGURE 25.—Variation of difference in pitching-moment coefficients of airplane and model ΔC_m (body axes) with angle of attack.

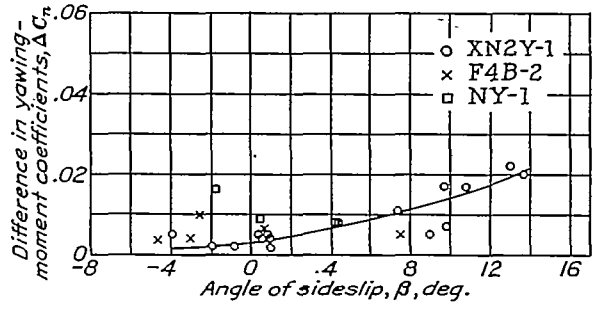

FIGURE 26.—Variation of difference in yawing-moment coefficients of airplane and model ΔC_n (body axes) with angle of sideslip.

The difference in pitching-moment coefficients ΔC_m shows no general variation with β or $\Omega b/2V$ but shows a slight tendency to decrease as α is increased (fig. 25). The average value of the difference is 0.02. The values of ΔC_m from the results obtained with the F4B–2 and the NY–1 airplanes are not sufficiently accurate for comparison.

The difference in yawing-moment coefficients ΔC_n shows no consistent variation with α or $\Omega b/2V$ but increases as β is increased (fig. 26). The difference is about 0.005 at slightly negative values of β, increasing to 0.02 at 13° sideslip. The values for the NY–1 and F4B–2 airplanes are included for comparison.

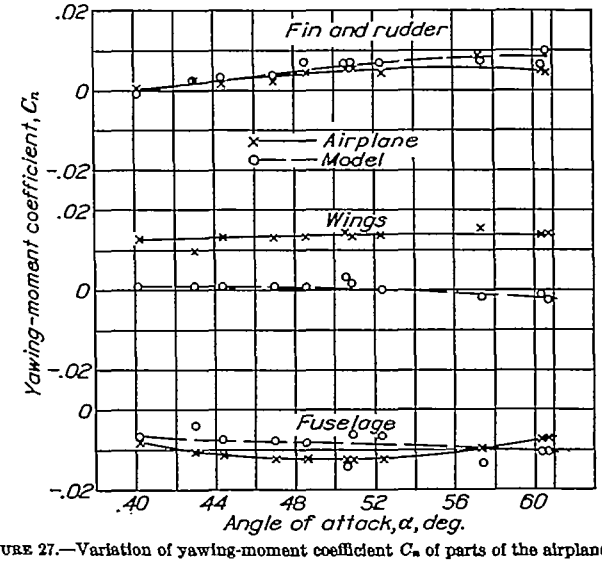

FIGURE 27.—Variation of yawing-moment coefficient C_n of parts of the airplane and parts of the model with angle of attack. (Full-scale results from reference 2.)

The values of C_n for the fin and rudder were obtained from the difference in the results obtained from the tests of the complete model and of the model with the fin and the rudder removed. The difference between flight results (reference 2) and model results changes from zero at 40° angle of attack to 0.003 at 60° (fig. 27). The values of C_n for the model wings with the struts and the attachment to the balance are about zero, while those for the airplane wings are about 0.013. Undoubtedly this difference is largely due to scale effects, which may normally be expected. The values of C_n for the model fuselage were obtained from the results of tests with the wings removed from the model

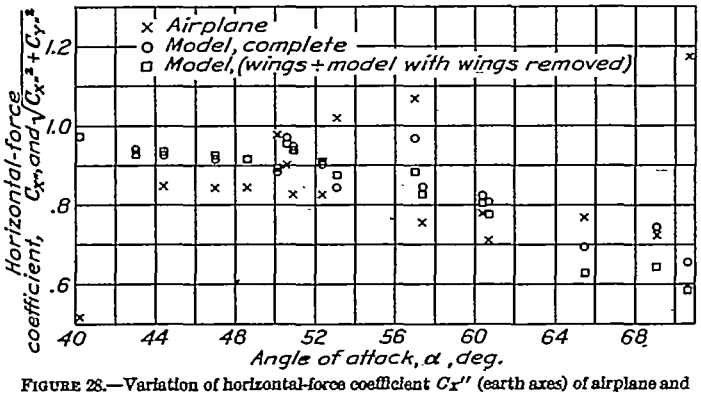

FIGURE 28.—Variation of horizontal-force coefficient $C_{X''}$ (earth axes) of airplane and of resultant-force coefficient $\sqrt{C_{X''^2}+C_{Y''^2}}$ (earth axes) of the model with angle of attack.

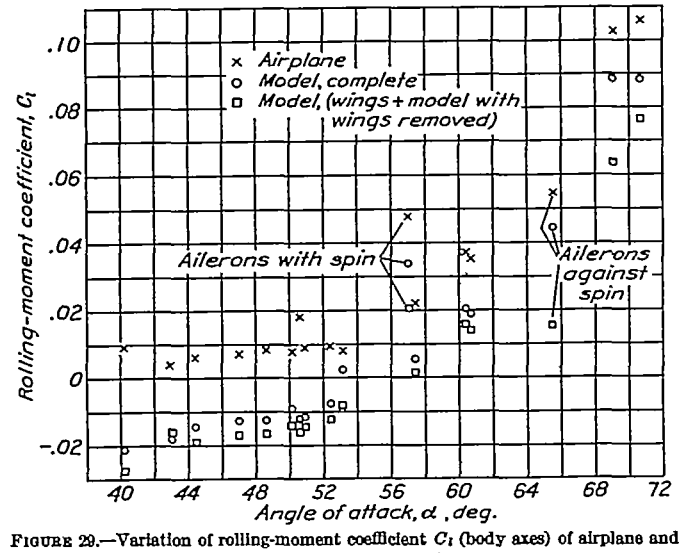

FIGURE 29.—Variation of rolling-moment coefficient C_l (body axes) of airplane and model with angle of attack.

minus the values obtained for the fin and rudder and are about the same as those obtained in flight at 40° and 55° angle of attack. Below 58° the values for the model are more positive and, above 58°, they are more negative than those obtained in flight.

The yawing moments for parts of the airplane were obtained in flight from pressure-distribution measurements on the important fuselage and tail-surface areas; the measurements included the interference of all parts of the airplane. The spinning-balance results were measured without the interference of some parts. This difference in method of measurement should give some difference other than that due to scale effects in the results and was intended to determine the scale and interference effects so that data for individual parts of models might be combined to give the characteristics of the complete model or airplane. The results of this part of the investigation are not sufficiently complete to draw definite conclusions because only one airplane is represented. It does, however, give some indication of the magnitude of the scale and interference effects that may be expected.

The interference effects caused by testing the wings alone and the model with wings removed for all the

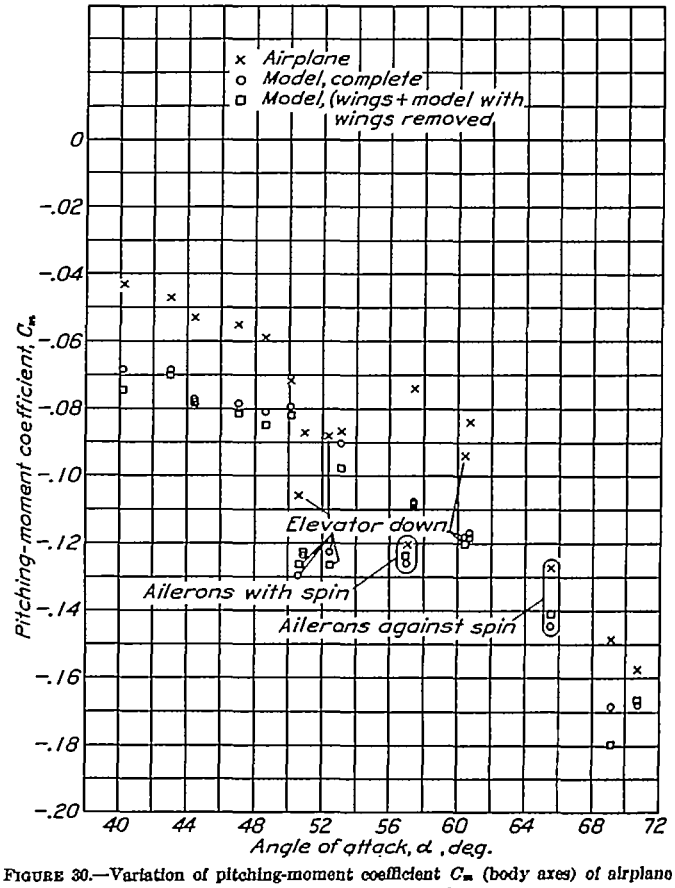

FIGURE 30.—Variation of pitching-moment coefficient C_m (body axes) of airplane and model with angle of attack.

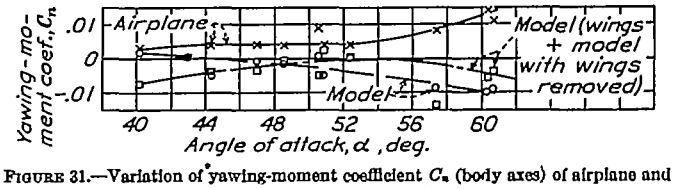

FIGURE 31.—Variation of yawing-moment coefficient C_n (body axes) of airplane and model with angle of attack.

coefficients, together with the values obtained for the airplane, are given in figures 28 to 31. At the higher angles of attack the values of $\sqrt{C_{X''^2}+C_{Y''^2}}$ for the complete model show a tendency to be greater than for the sum of the parts (fig. 28). The values of C_l for the complete model are generally more positive, by about 0.005, than the sum of the parts (fig. 29). The interference effect on C_m is small (fig. 30). The values of C_n for the sum of the parts are more negative than the values for the complete model below 49° angle of attack; above 49° the effect is reversed (fig. 31).

ANALYSIS OF DATA

DERIVATION OF EQUATIONS USED IN COMPUTING THE SPINNING ATTITUDE FROM SPINNING-BALANCE DATA

Since the necessary condition for a steady spin is that the aerodynamic forces and moments must exactly oppose the weight, centrifugal force, and inertia moments of the airplane, the following relations may be written.

(Because the resultant force on an airplane is not necessarily perpendicular to the XY plane of the airplane, as it was assumed to be in the computation of the attitudes, the computed azimuth setting of the model on the balance had the effect of rotating the resultant-force vector in the horizontal plane so that $C_{Y''}$ was not zero. Since $C_{Y''}$ must be zero in a steady spin and the resultant force in the horizontal plane must be exactly opposed by the centrifugal force, the resultant-force coefficient $\sqrt{C_{X''}^2+C_{Y''}^2}$ is used instead of $C_{X''}$ as might normally be expected.)

$$1/2\rho V^2 S C_{Z''}=mg \tag{1}$$

$$1/2\rho V^2 S\sqrt{C_{X''}^2+C_{Y''}^2}=m\Omega^2 R \tag{2}$$

$$1/2\rho V^2 SbC_m=1/2\Omega^2(A-C)\sin 2\alpha\cos^2(\sigma+\beta) \text{ nearly} \tag{3}$$

$$1/2\rho V^2 SbC_l=\Omega^2(C-B)\sin\alpha\sin(\sigma+\beta)\cos(\sigma+\beta) \text{ nearly} \tag{4}$$

$$1/2\rho V^2 SbC_n=\Omega^2(B-A)\cos\alpha\cos(\sigma+\beta)\sin(\sigma+\beta) \text{ nearly} \tag{5}$$

where σ is the angle between the vertical and the helix described by the center of gravity of the airplane. Relation (3) may be rewritten as

$$\frac{\Omega b}{2V}=\sqrt{\frac{-C_m}{4\mu\sin 2\alpha\cos^2(\sigma+\beta)}\times\left(\frac{b^2}{k_Z^2-k_X^2}\right)} \tag{6}$$

where $\mu=\dfrac{m}{\rho Sb}$ and $\left(\dfrac{b^2}{k_Z^2-k_X^2}\right)=\dfrac{Wb^2}{g(C-A)}$

Dividing relation (4) by (3) gives

$$C_l=-C_m\frac{k_Z^2-k_Y^2}{k_Z^2-k_X^2}\frac{\tan(\sigma+\beta)}{\cos\alpha} \tag{7}$$

where $$\frac{k_Z^2-k_Y^2}{k_Z^2-k_X^2}=\frac{C-B}{C-A}$$

Dividing relation (5) by (4) gives

$$C_n=C_l\cot\alpha\left(\frac{k_Y^2-k_X^2}{k_Z^2-k_Y^2}\right) \tag{8}$$

where $$\left(\frac{k_Y^2-k_X^2}{k_Z^2-k_Y^2}\right)=\frac{B-A}{C-B}$$

$$\sin\sigma=\frac{\Omega R}{V} \text{ from definition} \tag{9}$$

$$\sin\sigma=\frac{\sqrt{C_{X''}^2+C_{Y''}^2}}{4\mu\dfrac{\Omega b}{2V}} \text{ from (2) and (9)} \tag{10}$$

COMPUTED SPINNING EQUILIBRIUM

1. The value of σ is obtained for each test condition by using equation (10).

2. The value of $\Omega b/2V$ required for balance of the aerodynamic and inertia pitching moments is computed from equation (6) for each test condition, C_m being increased by 0.02 for reasons given in the text. These computed values of $\Omega b/2V$ and the values used in testing the model were plotted against C_m. (See fig. 32.) The intersection of these curves gives the equilibrium values of $\Omega b/2V$ and C_m for each angle of attack at each angle of sideslip tested.

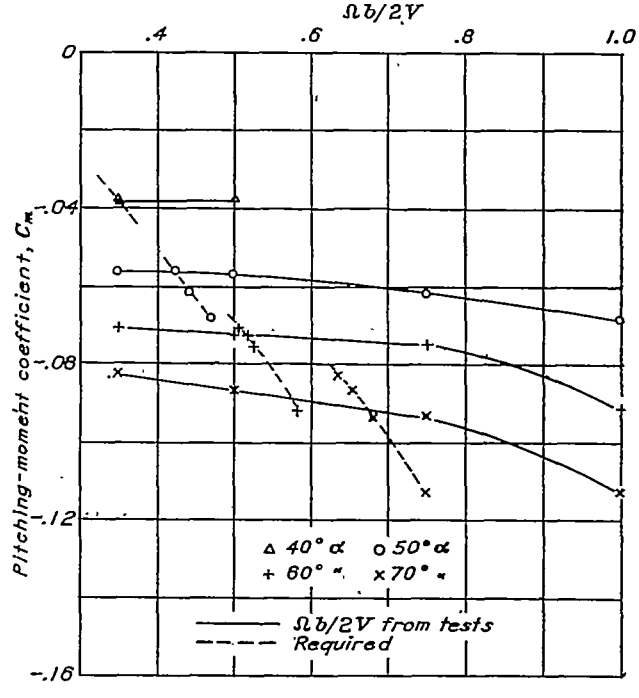

FIGURE 32.—Variation of pitching-moment coefficient C_m (body axes) with $\Omega b/2V$ (Value of $\Omega b/2V$ from tests.) $\beta=-10°$.

3. The value of the rolling moment required for equilibrium with the inertia moment is found from equation (7) by using the values of C_m and σ that gave a balance of pitching moments (par. 2). These rolling moments, and those from the test data, increased by 0.02, are plotted against β for each angle of attack in figure 33. Intersection of these curves gives values of β and C_l for spinning equilibrium at each angle of attack tested.

4. The values of the aerodynamic yawing moment required for equilibrium are obtained from equation (8) by using the value of C_l found from paragraph 3,

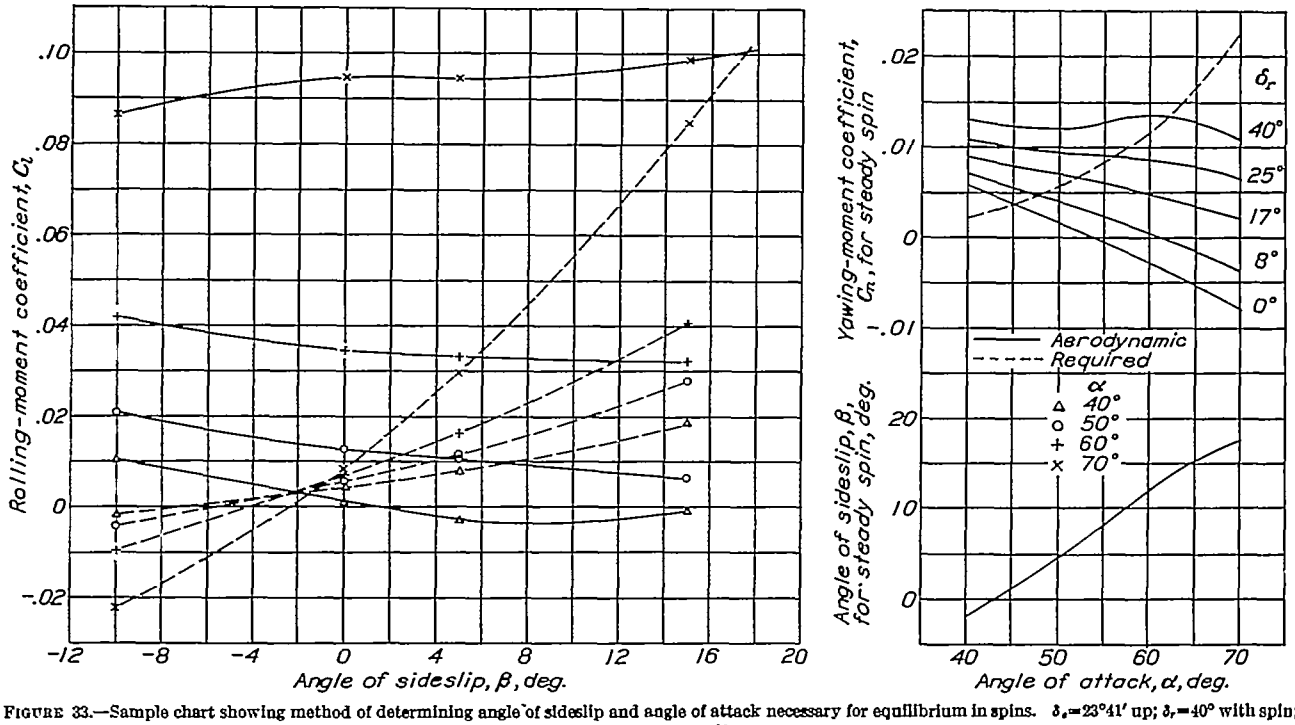

FIGURE 33.—Sample chart showing method of determining angle of sideslip and angle of attack necessary for equilibrium in spins. δ_a=23°41′ up; δ_r=40° with spin; μ=4.74; $\frac{k_x^2-k_y^2}{k_z^2-k_x^2}$=0.616; $\frac{b^2}{k_z^2-k_x^2}$=59.3.

and those obtained from the data (changed according to fig. 26 for full-scale) at corresponding conditions are plotted against angle of attack (fig. 33). Equilibrium in a spin is indicated where these curves intersect.

5. The value of $\Omega b/2V$ for the attitude found by the method of paragraph 4 is determined in the following way: Plot the aerodynamic rolling moments required, computed for each angle of attack from paragraph 3, against $\Omega b/2V$, from which the value of $\Omega b/2V$ for each angle of attack can be found, since the value of C_l for equilibrium has been obtained in paragraph 3. (Fig. 34 is a sample chart.) Plot these values of $\Omega b/2V$ against α and, since the value of α of the spin is known from paragraph 4, the value of $\Omega b/2V$ for the indicated spin is obtained.

This method of analysis is essentially the same as that given in reference 8, modified for use with the data from the complete model instead of from only the wing.

INDEPENDENT VARIABLES USED IN COMPUTATIONS

Computations for estimations of spin characteristics were made for assumed characteristics of the airplane for comparison with flight results, and are tabulated in table II.

Table III gives the assumed airplane characteristics that were used to estimate spins for a comparison with the results from the free-spinning tunnel. A model made to the same dimensions as the model tested on the spinning balance and with these same parameters was tested in the free-spinning tunnel.

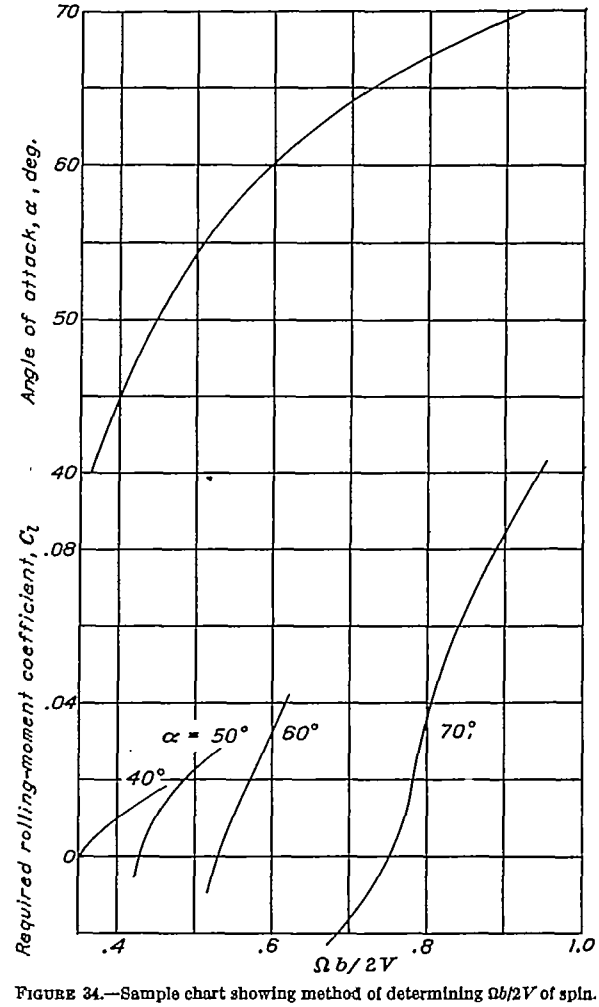

FIGURE 34.—Sample chart showing method of determining $\Omega b/2V$ of spin.

TABLE II.—AIRPLANE PARAMETERS

μ	$\frac{b^2}{k_Z^2-k_X^2}$	$\frac{k_Z^2-k_Y^2}{k_Z^2-k_X^2}$	δ_a (deg.)	δ_e[1] (deg.) (min.)	δ_r[2] (deg.)
2.5	70	1.00	0	−23 41	−40
4.5	70	1.00	0	−23 41	−40
7.5	70	1.00	0	−23 41	−40
10.0	70	1.00	0	−23 41	−40
4.5	50	1.00	0	−23 41	−40
4.5	90	1.00	0	−23 41	−40
4.5	110	1.00	0	−23 41	−40
4.5	70	.50	0	−23 41	−40
4.5	70	1.50	0	−23 41	−40
4.5	70	2.00	0	−23 41	−40
4.5	70	2.50	0	−23 41	−40
4.5	70	1.00	[3] Against	−23 41	−40
4.5	70	2.00	Against	−23 41	−40
4.5	70	1.00	[4] With	−23 41	−40
4.5	70	2.00	With	−23 41	−40
4.74	69.30	.616	0	−23 41	−40
[5]3.91	60.90	.718	0	−23 41	−40
4.74	73.73	2.0	0	25 0	40
4.74	73.73	2.5	0	25 0	40
4.74	73.73	2.0	0	0 0	0
4.74	73.73	2.5	0	0 0	0
7.5	70	2.0	0	0 0	0
7.5	70	1.0	0	0 0	0
7.5	70	2.0	0	25 0	40
7.5	70	1.0	0	25 0	40

[1] Positive when elevators are down.
[2] Positive in a right spin when rudder is against spin.
[3] Right aileron up 25°, left aileron down 15°.
[4] Left aileron up 25°, right aileron down 15°.
[5] Corresponds to flight tests 38L, 40L, and 41L of reference 1.

TABLE III.—SPIN-TUNNEL PARAMETERS

μ	$\frac{b^2}{k_Z^2-k_X^2}$	$\frac{k_Z^2-k_Y^2}{k_Z^2-k_X^2}$	δ_a (deg.)	δ_e (deg.) (min.)	δ_r (deg.)
4.80	62.00	0.558	0	−23 41	−40
4.90	63.00	.853	0	−23 41	−40
5.00	64.49	1.147	0	−23 41	−40
5.09	65.76	1.440	0	−23 41	−40
5.19	67.03	1.734	0	−23 41	−40
6.16	79.55	.558	0	−23 41	−40
7.52	97.13	.558	0	−23 41	−40
7.52	97.13	.558	0	0 0	0
7.52	97.13	.558	0	25 0	40
7.52	97.13	1.734	0	0 0	0
7.52	97.13	1.734	0	25 0	40

Under standard conditions at sea level for this airplane, values of μ of 2.5 and 10 correspond to wing loadings of 5.36 and 21.46 pounds per square foot, respectively. The variables used were chosen to cover the range for all wing loadings and moments of inertia likely to be used with an airplane of this type and included some specific values used in flight and in the free-spinning tunnel.

The results of the analyses are given in figures 35 to 40. Each analysis, with $\delta_e=23°41'$ up, was computed, in addition to $\delta_r=40°$ with, for rudder settings of 25°, 17°, 8°, and 0° by using the values of C_n given in figure 22 and by assuming that the only effect of moving the rudder from 40° with the spin was to change C_n and that the value of $\Omega b/2V$ was 0.75 at $\alpha=60°$ and 0.50 at $\alpha=50°$. These assumptions are only approximate because C_n changes considerably with $\Omega b/2V$ (see fig. 15) and C_m changes with rudder movement. The results are included because they indicate the general effects of rudder deflections.

ARBITRARY CORRECTIONS TO SPINNING-BALANCE DATA USED IN MAKING THE ANALYSIS

Full-scale.—Previous investigations (references 4 and 5) and figures 23 to 26 indicate that it is necessary to correct spinning-balance data when estimating spins. No correction to $C_{X''}$ is considered necessary because $\Delta C_{X''}$ is a small percentage of $C_{X''}$ and rather large values of $\Delta C_{X''}$ would make but small differences in estimating spins. The average value of 0.02 has been added to C_l and C_m because ΔC_l and ΔC_m show only slight tendencies to vary with α, β, or $\Omega b/2V$, and the individual points are scattered. All C_n values were changed by the amount indicated by the curve (fig. 26) for this analysis because the curve of ΔC_n against β is well defined and the differences are sufficiently large to cause large angle-of-attack differences in the estimated spin.

Free-spinning tunnel.—If the differences between spinning-balance and flight results were all due to scale effect, then steady spins estimated from uncorrected balance data should agree with those obtained in the free-spinning tunnel. However, the values of $\Omega b/2V$ obtained from tests in flight and in the free-spinning tunnel (references 2 and 3) are very nearly the same and, since C_m determines to a large extent the curve of $\Omega b/2V$ against α (fig. 34), a correction of 0.02 was applied to C_m for all estimations of spins used for comparison with the results from the free-spinning tunnel.

DISCUSSION OF RESULTS OF ANALYSIS

ESTIMATED FULL-SCALE ATTITUDES

Increasing μ increases the angle of attack, makes the sideslip more positive, and increases the values of $\Omega b/2V$ when the rudder is 25° or more with the spin (fig. 35). In general, it appears that increased wing loadings and higher altitudes would make the spin flatter and recoveries slower and more difficult.

Increasing the pitching-moment inertia parameter $b^2/(k_Z^2-k_X^2)$ (decreasing $C-A$) generally decreases the angle of attack, makes the sideslip more outward (negative in a right spin), and does not appreciably change $\Omega b/2V$ (fig. 36). The effect on time for recovery of changing $b^2/(k_Z^2-k_X^2)$ would probably be small.

Increasing the rolling- and yawing-moment inertia parameter $(k_Z^2-k_Y^2)/(k_Z^2-k_X^2)$, i. e., moving weight from the center of gravity out along the wings (fig. 37), increases the angle of attack and $\Omega b/2V$ and makes the sideslip more nearly zero. Increasing this parameter would apparently make the airplane spin faster and flatter with recoveries probably slower and more difficult.

This analysis indicates that a large value of μ and a large value of $(k_Z^2-k_Y^2)/(k_Z^2-k_X^3)$ would make the airplane spin at high angles of attack and very fast. It was thought that large values of these parameters might produce spins with the controls neutral or against the spin. Accordingly, analyses were made with $\mu=7.5$, $b^2/(k_Z^2-k_X^2)=70$, $(k_Z^2-k_Y^2)/(k_Z^2-k_X^2)=1.0$ and 2.0, and tail surfaces both neutral and against the spin; but in no case was a spin indicated. Approximately the same conditions were tried in the free-spinning tunnel with the same results.

Moving the rudder, with elevators up, any amount from full with the spin to neutral in all cases reduces the angle of attack and $\Omega b/2V$ and makes the sideslip more outward.

Equilibrium was impossible in every case in a spin analyzed with elevator and rudder neutral or both against the spin. Moving the ailerons from against the spin to with the spin (fig. 38) decreases the angle of attack and decreases $\Omega b/2V$ with elevators up and this analysis are shown in figure 39. The estimated spins agree very well with flight results when $(k_Z^2-k_Y^2)/(k_Z^2-k_X^2)$ is equal to 1.4. For other values of this parameter the disagreement between the results is considerable. When $(k_Z^2-k_Y^2)/(k_Z^2-k_X^2)$ is equal to 0.718, the only condition flight-tested both to the right and left, the flight results are generally greater or less than those obtained from analysis, depending upon whether the airplane was spun to the right or to the

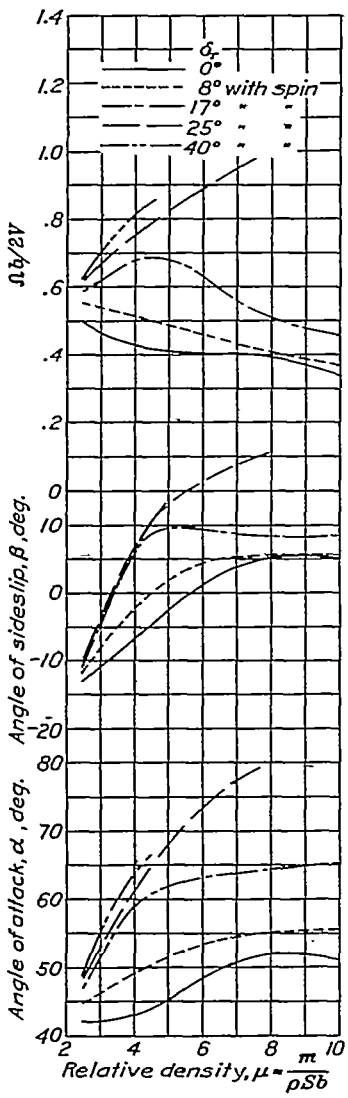

FIGURE 35.—Variation of estimated values of angle of attack, angle of sideslip, and $\Omega b/2V$ with relative density of airplane. δ_a=0°; δ_e=23°41′ up; $\frac{k_Z^2-k_Y^2}{k_Z^2-k_X^2}$=1.0; $\frac{b^2}{k_Z^2-k_X^2}$=70.

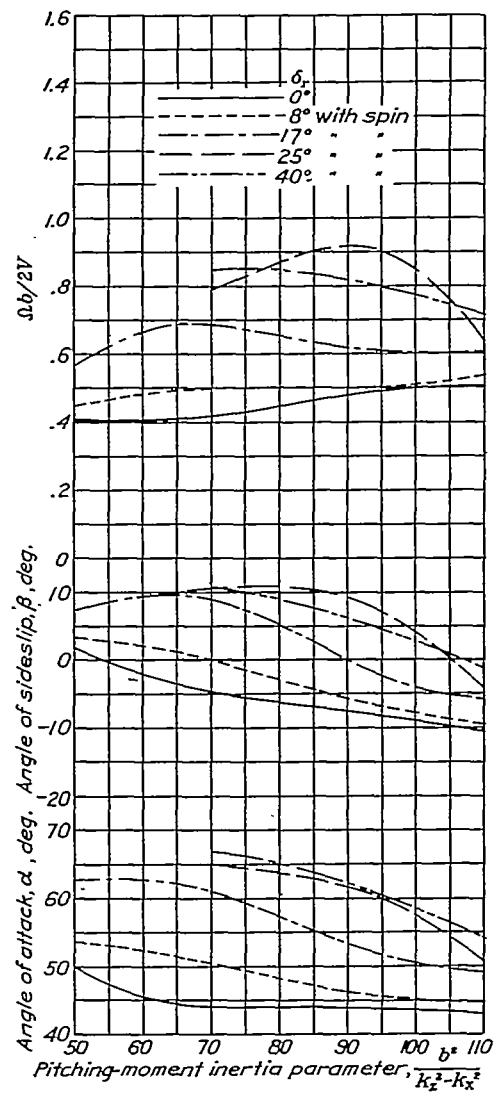

FIGURE 36.—Variation of estimated values of angle of attack, angle of sideslip, and $\Omega b/2V$ with pitching-moment inertia parameter $\frac{b^2}{k_Z^2-k_X^2}$. δ_a=0°; δ_e=23°41′up; μ=4.5; $\frac{k_Z^2-k_Y^2}{k_Z^2-k_X^2}$=1.0.

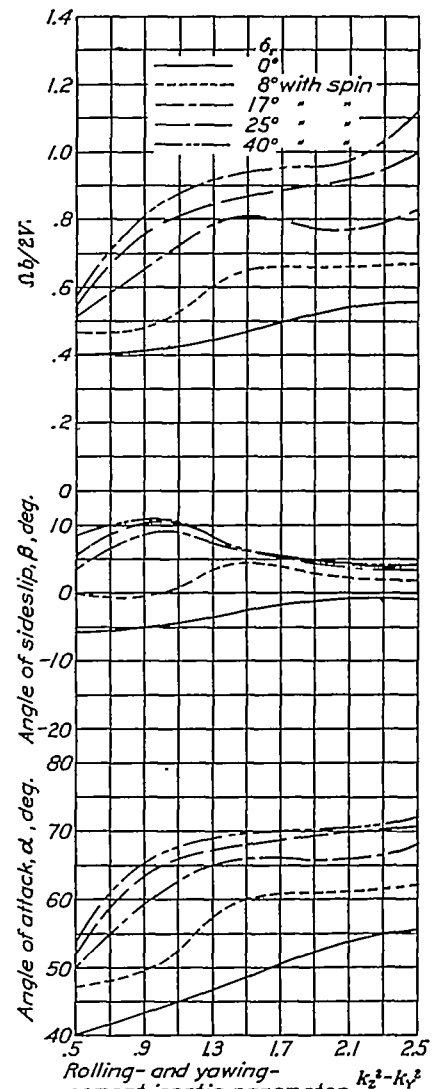

FIGURE 37.—Variation of estimated values of angle of attack, angle of sideslip, and $\Omega b/2V$ with rolling- and yawing-moment inertia parameter $\frac{k_Z^2-k_Y^2}{k_Z^2-k_X^2}$. δ_a=0°; δ_e=23°41′ up; μ=4.5; $\frac{b^2}{k_Z^2-k_X^2}$=70.

rudder full with the spin. With other rudder settings this effect is reduced and, with δ_r=0° and $(k_Z^2-k_Y^2)/(k_Z^2-k_X^2)$=2.0, the angle of attack and $\Omega b/2V$ are increased. Ailerons moved from against the spin to with the spin generally tend to increase the sideslip and make the values more nearly the same for all rudder settings.

COMPARISON WITH FULL-SCALE RESULTS

An analysis for estimation of spins was made for some flight conditions given in reference 1. The results of left. There is no doubt but that part of this difference is due to dissymmetry of the airplane used in the flight tests. The results of the one test with wing-tip ballast show considerably different aerodynamic characteristics than do the results of the tests without ballast (reference 2); this discrepancy, however, may be due to the changing of the period of vibration of the wings by the ballast, thus affecting the rolling and yawing moments. At the beginning of these tests on the spinning balance it was found that, under certain conditions,

the rolling moment (for earth axes) could be varied as much as 100 percent by changing the tension of a spring attached to the rolling-moment arm in the balance. When the rigidity of the wings with respect to the fuselage was increased, this variation in moment with spring tension completely disappeared. There can be little doubt that this variation was aerodynamic because the balance was carefully checked and a corresponding condition has been observed in which the setting of zero is very questionable, as previously explained, and therefore will not be discussed.

The angle of sideslip for rudder settings of 40° and 17° with the spin is generally within the limits of error (a degree or so) of the results obtained in the free-spinning tunnel.

The values of C_n are usually 0.001 to 0.003 too low to give the angle of attack obtained from the free-spinning tunnel. This difference indicates that the results from

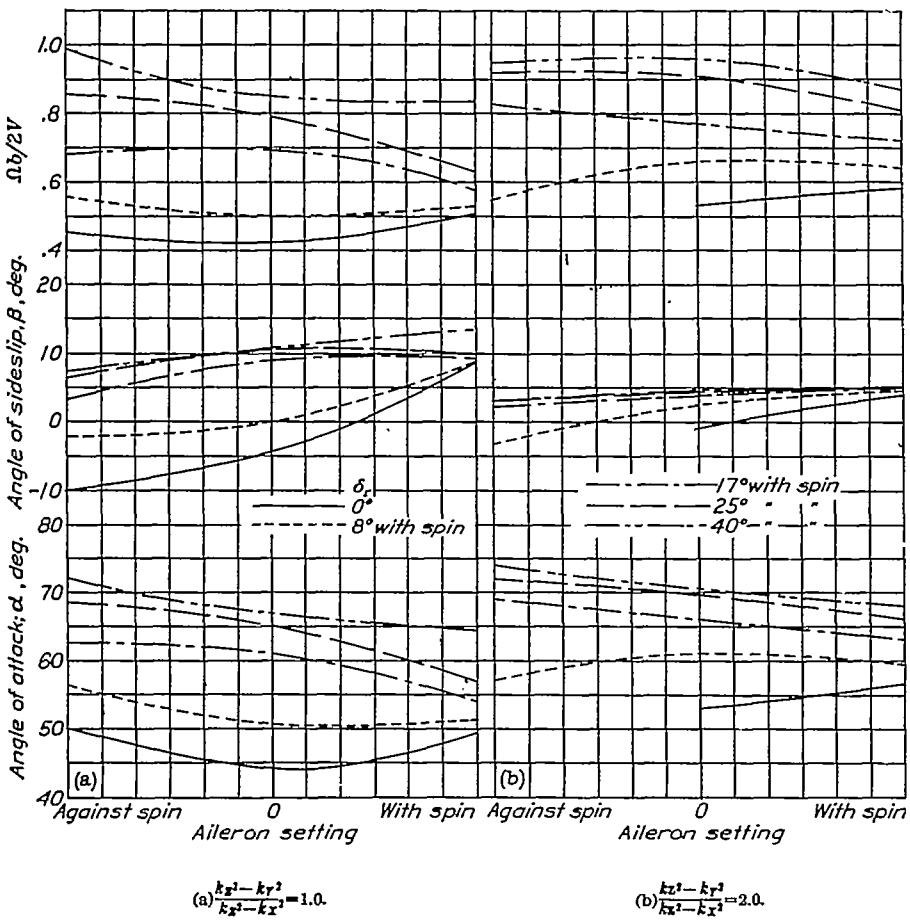

(a) $\frac{k_z^2-k_Y^2}{k_x^2-k_X^2}=1.0$. (b) $\frac{k_z^2-k_Y^2}{k_x^2-k_X^2}=2.0$.

FIGURE 38.—Variation of estimated values of angle of attack, angle of sideslip, and $\Omega b/2V$ with aileron setting. $\delta_e=23°41'$ up; $\mu=4.5$; $\frac{b^3}{k_x^2-k_X^2}=70$.

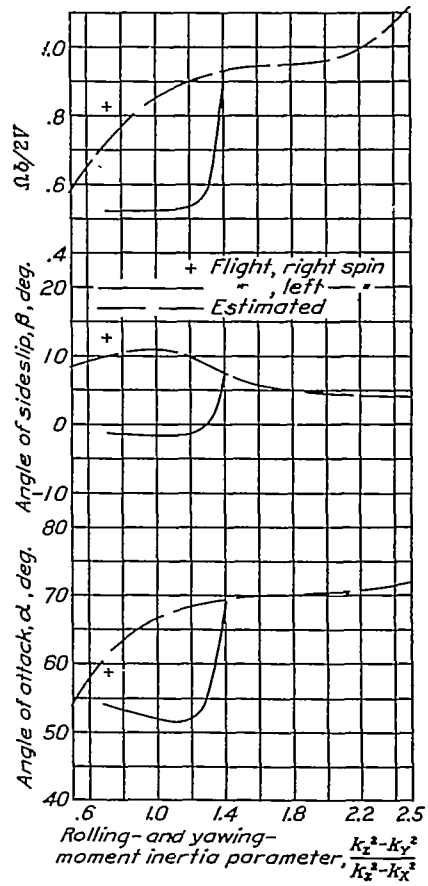

FIGURE 39.—Variation of flight and estimated values of angle of attack, angle of sideslip, and $\Omega b/2V$ with rolling- and yawing-moment inertia parameter $\frac{k_z^2-k_Y^2}{k_x^2-k_X^2}$. $\delta_e=0°$; $\delta_a=23°41'$ up; $\delta_r=40°$ with spin $\mu=4.5$; $\frac{b^3}{k_x^2-k_X^2}=70$.

tail surfaces and wings of a model vibrated during routine tests in another wind tunnel.

COMPARISON WITH RESULTS FROM THE FREE-SPINNING TUNNEL

The results of the analysis and results of tests from the free-spinning tunnel are given in figure 40. The estimated values of β, $\Omega b/2V$, and C_n necessary for equilibrium in a steady spin are plotted against the angle of attack; the values obtained from the free-spinning tunnel were obtained from reference 3 and from unpublished data. The results agree fairly well except below 40° angle of attack, in which range the model could not be tested on the spinning balance because of interference with the balance. The extrapolation of the spinning-balance data for the rudder the free-spinning tunnel are slightly more positive than those obtained from the spinning balance; however, this discrepancy may be an indication that the correction of 0.02 to the pitching moment was not large enough, since increasing the value of the correction reduces the difference.

The fact that the values of $\Omega b/2V$ are usually slightly lower than those obtained from the free-spinning tunnel also indicates that a correction to C_m of the order of 0.021 or 0.022 would have given slightly better agreement for both $\Omega b/2V$ and C_n.

The agreement between spins as estimated from results obtained from the spinning balance and from those obtained from the free-spinning tunnel is generally well within the limits of error except for the necessary correction to C_m.

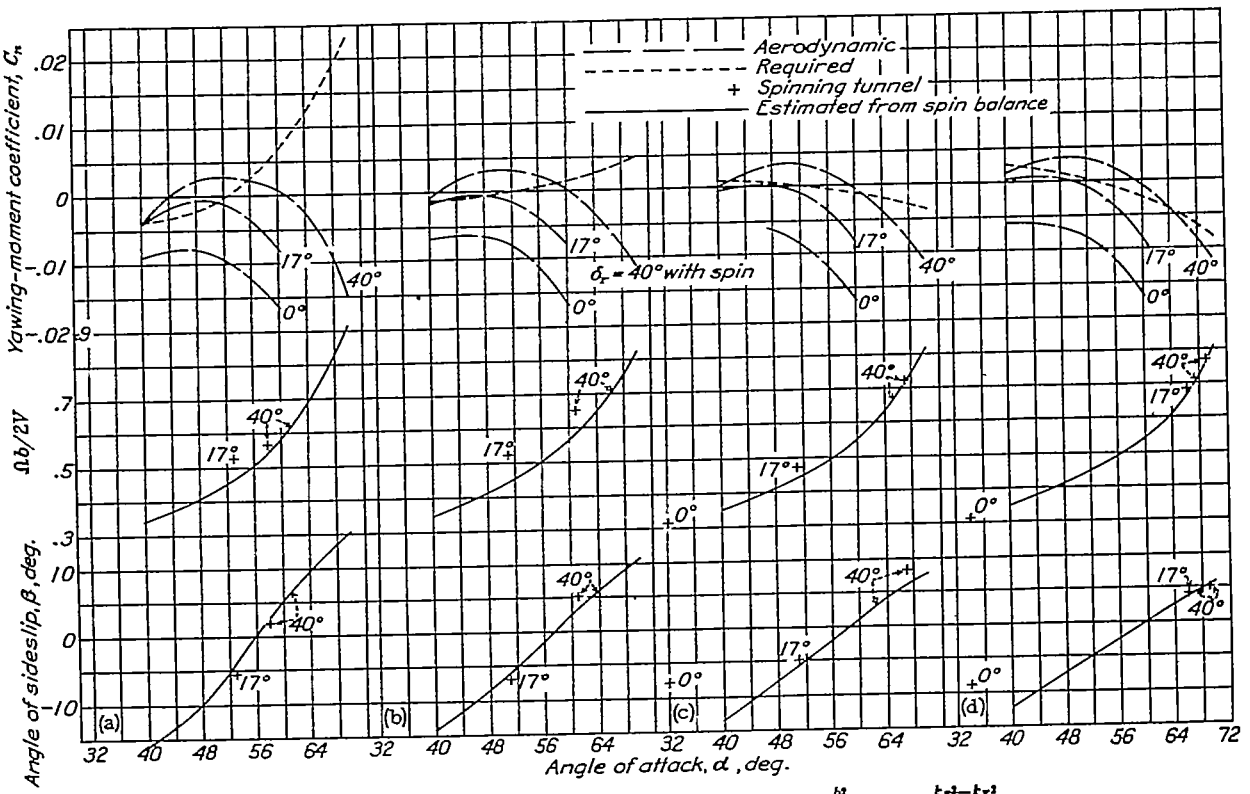

(a) $\mu=4.8$; $\frac{b^2}{k_Z^2-k_X^2}=62$; $\frac{k_Z^2-k_Y^2}{k_Z^2-k_X^2}=0.553$.

(b) $\mu=4.9$; $\frac{b^2}{k_Z^2-k_X^2}=63.3$; $\frac{k_Z^2-k_Y^2}{k_Z^2-k_X^2}=0.853$.

(c) $\mu=5.0$; $\frac{b^2}{k_Z^2-k_X^2}=64.49$; $\frac{k_Z^2-k_Y^2}{k_Z^2-k_X^2}=1.147$.

(d) $\mu=5.09$; $\frac{b^2}{k_Z^2-k_X^2}=65.76$; $\frac{k_Z^2-k_Y^2}{k_Z^2-k_X^2}=1.44$.

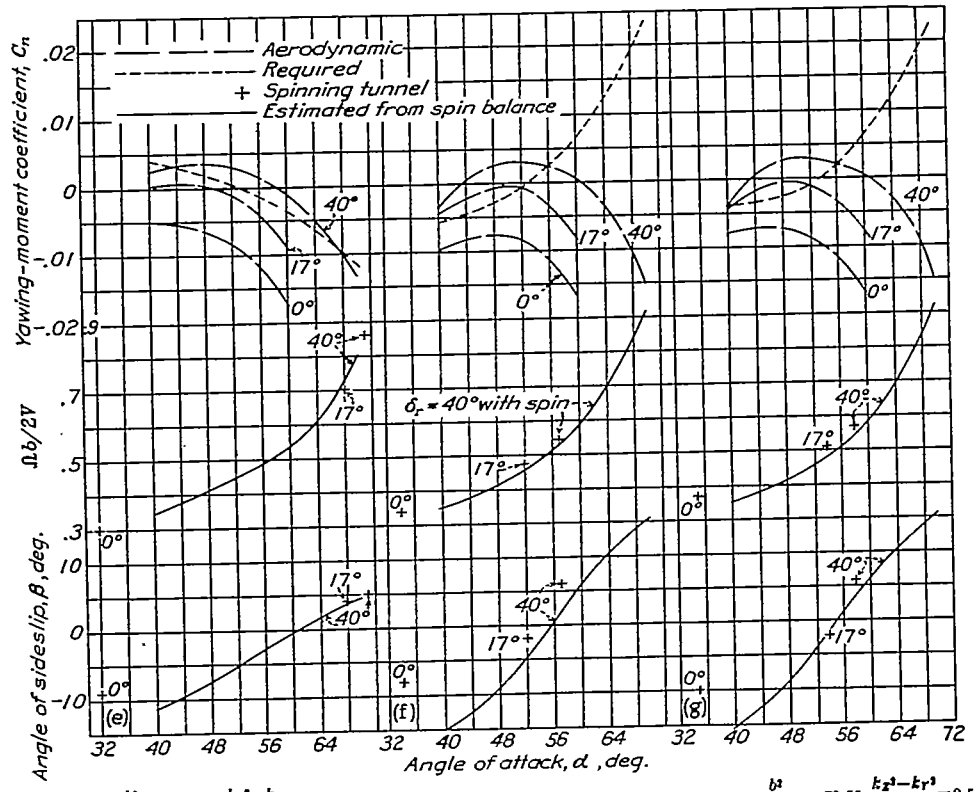

(e) $\mu=5.19$; $\frac{b^2}{k_Z^2-k_X^2}=67.03$; $\frac{k_Z^2-k_Y}{k_Z^2-k_X}=1.734$.

(f) $\mu=6.16$; $\frac{b^2}{k_Z^2-k_X^2}=79.55$; $\frac{k_Z^2-k_Y^2}{k_Z^2-k_X^2}=0.558$.

(g) $\mu=7.52$; $\frac{b^2}{k_Z^2-k_X^2}=97.13$; $\frac{k_Z^2-k_Y^2}{k_Z^2-k_X^2}=0.558$.

FIGURE 40.—Variation of angle of sideslip, yawing-moment coefficient, and $\Omega b/2V$ with angle of attack. $\delta_a=0°$; $\delta_e=23°41'$ up.

COMPARISON OF SPINS OBTAINED IN THE FREE-SPINNING TUNNEL WITH THOSE OBTAINED IN FLIGHT AS INDICATED BY THE SPINNING-BALANCE DATA

The comparison of spins in flight and in the free-spinning tunnel is based on the necessary corrections to the data obtained from the spinning balance to give agreement with results from flight and from the free-spinning tunnel.

The differences in $C_{X''}$ (force coefficient in the horizontal plane) and in C_m are not large enough to have an appreciable effect on the results. The effect of changes in $C_{X''}$ have been shown in references 7 and 8 and the changes in C_m have been discussed in this report.

If an arbitrary constant of 0.02 could be added to the C_l for tests in the free-spinning tunnel, the sideslip of the model and the airplane should be about the same. The differences in yawing moments are but slightly less than those given in figure 26. In the comparison of spins, however, the difference in yawing moment required caused by the difference in sideslip between the model and the airplane must be considered.

The effect of sideslip on the yawing moment required is reflected as a change in C_l in equation (8):

$$C_n = C_l \cot \alpha \left(\frac{B-A}{C-B}\right)$$

For the model of the XN2Y–1 airplane, C_l would always be about 0.02 less than for the full-scale airplane because the aerodynamic rolling moment does not change much with β. (See fig. 33.) If $(B—A)$ is positive, the value of C_n required for the model will always be less than for the airplane, which gives (in the analysis) the same effect as adding an increment to the aerodynamic yawing moment available. The result of this counteracting effect is that the model may spin at the same angle of attack and recover in much the same manner as the airplane. When $(B—A)$ is negative, this effect will be reversed and greater discrepancies between model and airplane spins may be expected. Also, the aerodynamic yawing moment may be considerably different because of the difference in sideslip between the model and the airplane, since the yawing-moment coefficient varies with angle of sideslip. (See figs. 12 and 22.) The inference from these comparisons is that the free-spinning tunnel will, for certain airplanes, give reasonable indications of the behavior of the airplane in the spin but in other cases the behavior of the model and of the airplane may be considerably different.

CONCLUSIONS

1. Scale effects on models, and tunnel and oscillation effects on the spinning-balance results, make it difficult to estimate the equilibrium attitude in a full-scale spin.

2. For the XN2Y–1 airplane the differences in C_l and C_n between full-scale and spinning-balance results agree with the differences found for two other airplanes previously tested. No comparisons of C_m can be made with previous results because of the inaccuracy of this value in the earlier tests.

3. An average difference of 0.02 was found in C_l and C_m between flight results and spinning-balance results. The differences in C_n were found to increase with β as β became more positive (more inward sideslip in a right spin). The value of C_n was found to be about 0.005 at slightly negative values of sideslip, increasing to 0.02 at 13° positive sideslip.

4. Good agreement for steady-spinning attitudes between results from the free-spinning tunnel and estimations of spins from spinning-balance data can be obtained by adding 0.02 to the values of the pitching-moment coefficients measured with the spinning balance.

5. This investigation indicates that good agreement in the attitude for steady spins between results from full-scale tests and those from the free-spinning tunnel can be obtained by adding 0.02 to the model rolling-moment coefficient and an increment that depends on the angle of sideslip to the model yawing-moment coefficient.

LANGLEY MEMORIAL AERONAUTICAL LABORATORY,
NATIONAL ADVISORY COMMITTEE FOR AERONAUTICS,
LANGLEY FIELD, VA., *April 16, 1937.*

REFERENCES

1. Scudder, N. F.: A Flight Investigation of the Effect of Mass Distribution and Control Setting on the Spinning of the XN2Y–1 Airplane. T. R. No. 484, N. A. C. A., 1934.
2. Scudder, N. F.: The Forces and Moments Acting on Parts of the XN2Y–1 Airplane During Spins. T. R. No. 559, N. A. C. A., 1936.
3. Zimmerman, C. H.: Preliminary Tests in the N. A. C. A. Free-Spinning Wind Tunnel. T. R. No. 557, N. A. C. A., 1936.
4. Bamber, M. J., and Zimmerman, C. H.: The Aerodynamic Forces and Moments Exerted on a Spinning Model of the NY–1 Airplane as Measured by the Spinning Balance. T. R. No. 456, N. A. C. A., 1933.
5. Bamber, M. J., and Zimmerman, C. H.: The Aerodynamic Forces and Moments on a Spinning Model of the F4B–2 Airplane as Measured by the Spinning Balance. T. N. No. 517, N. A. C. A., 1935.
6. Wenzinger, Carl J., and Harris, Thomas A.: The Vertical Wind Tunnel of the National Advisory Committee for Aeronautics. T. R. No. 387, N. A. C. A., 1931.
7. Bamber, M. J.: Spinning Characteristics of Wings. II–Rectangular Clark Y Biplane Cellule: 25 Percent Stagger; 0° Decalage; Gap/Chord 1.0. T. N. No. 526, N. A. C. A., 1935.
8. Bamber, M. J., and Zimmerman, C. H.: Spinning Characteristics of Wings. I–Rectangular Clark Y Monoplane Wing T. R. No. 519, N. A. C. A., 1935.